UNCERTAINTIES 2012

Proceedings of the 1st International Symposium on Uncertainty Quantification and Stochastic Modeling
February 26th to March 2nd, 2012, Maresias, São Sebastião, SP, Brazil

PERFORMANCE OF ACTIVE AND PASSIVE VIBRATION CONTROL USING PIEZOELECTRIC MATERIALS SUBJECTED TO UNCERTAINTIES ON ELECTRICAL AND MATERIAL PROPERTIES

Heinsten F.L. Santos and Marcelo A. Trindade

[1] Department of Mechanical Engineering, São Carlos School of Engineering, University of São Paulo,
São Carlos, SP 13566-590, Brazil, hfleal@sc.usp.br

Abstract. *Piezoelectric materials can be used either as actuators connected to an appropriate control law to provide active vibration control or as sensors connected to shunt circuits to provide passive damping. In the last decade, research was redirected to combined active and passive vibration control techniques. One of these techniques, so-called Active-Passive Piezoelectric Networks (APPN), integrates an active voltage source with a passive resistance-inductance shunt circuit to a piezoelectric sensor/actuator. It has been shown that combined active-passive vibration control allows better performance with smaller cost than separate active and passive control, provided the simultaneous action is optimized. On the other hand, like for purely passive shunted piezoelectric damping, most of the studies concerning APPN focus on the optimization of the electric circuit architecture and components. In particular, a main issue for resonant shunt circuits is the high values of inductance needed when low frequency modes are to be controlled which normally requires the use of a synthetic inductance and, also, the need for a fine tuning of the circuit parameters with structural natural frequencies and electromechanical coupling coefficient. Another issue is the sensitivity of the control design and performance to the circuit components and structural natural frequencies. Some simple formulas were proposed for the quantification of the effect of resonant shunt circuits impedances uncertainties on the passive damping performance. This work presents an analysis of active-passive vibration control using APPN subject to parametric uncertainties in the shunt circuit components and piezoelectric material properties. This is done using a recently developed finite element model, which fully accounts for the structure/piezoelectric elements/circuits interaction, combined to stochastic modeling techniques to evaluate confidence intervals for the vibration control performance. Results for the first vibration mode of a cantilever beam with piezoceramic patches connected to active-passive shunt circuits are presented and discussed. In particular, the combination of active and passive control mechanisms and its effects on the control performance and its confidence intervals are discussed.*

Keywords. *Active-passive piezoelectric networks, uncertainties, piezoelectric materials, vibration control, resonant shunt circuits*

1 INTRODUCTION

Piezoelectric materials, and especially piezoelectric composites such as multilayered plates including active piezoelectric layers are excellent candidates for designing adaptive devices for shape and vibration control of elastic structures. Such devices and piezoelectric composites are of great technological interest in structural engineering with applications to noise reduction or shape control of large flexible structures. Most modellings of piezoelectric actuators or composites consider laminated structures made of continuous piezoelectric layers. This is due to their strong electromechanical coupling of the piezoelectric materials making widely used as sensors and actuators for structural vibration control. They can be used either as actuators connected to an appropriate control law to provide active vibration control or as sensors connected to shunt circuits to provide passive damping. In the last decade, research was redirected to combined active and passive vibration control techniques. One of these techniques, so-called Active-Passive Piezoelectric Networks (APPN), integrates an active voltage source with a passive resistance-inductance shunt circuit to a piezoelectric sensor/actuator (Tsai and Wang, 1999). In this case, the piezoelectric material serves two purposes. First, the vibration strain energy of the structure can be transferred to the shunt circuit, through the difference of electric potential induced in the piezoelectric material electrodes, and then passively dissipated in the electric components of the shunt circuit (Forward, 1979; Hagood and von Flotow, 1991, Viana and Steffen, 2006). On the other hand, the piezoelectric material may also serve as an actuator for which a control voltage can be applied to actively control the structural vibrations. This active mechanism combined to a velocity feedback, for instance, may then induce an additional active damping in the structure.

There are still some unresolved issues concerning this active-passive damping mechanism such as for which conditions simultaneous active-passive damping outperforms separate active and passive mechanisms, that is, whether the control voltage should be part of the shunt circuit or not (Thornburgh and Chattopadhyay, 2003). It has been shown that combined active-passive vibration control allows better performance with smaller cost than separate active and passive control, provided the simultaneous action is optimized (Tsai and Wang, 1999). On the other hand, like for purely passive shunted piezoelectric damping, most of the studies concerning APPN focus on the optimization of the electric circuit architecture and components. It is well-known however that the performance of both active and passive damping mechanisms is highly dependent on the effective electromechanical coupling provided by the piezoelectric actuators/sensors. Nevertheless, few

studies focus on the optimization of this coupling for given structure and piezoelectric material. In particular, it has been shown that piezoelectric actuators using their thickness-shear mode can be more effective than surface-mounted extension piezoelectric actuators for both active (Trindade, Benjeddou and Ohayon, 1999; Raja, Prathap and Sinha, 2002; Baillargeon and Vel, 2005; Trindade and Benjeddou, 2006) and passive (Benjeddou and Ranger-Vieillard, 2004; Benjeddou, 2007; Trindade and Maio, 2008) vibration damping. One of the reasons for that is the thickness-shear electromechanical coupling coefficient k_{15} that is normally twice the value of the extension one k_{31}, which may lead to a higher effective electromechanical coupling coefficient (Trindade and Benjeddou, 2009). The thickness-shear mode, originally proposed by Sun and Zhang (1995), can be obtained using longitudinally-poled piezoelectric patches that couple through-thickness electric fields/displacements and shear strains/stresses. On the other hand, although it is well-known that the performance of shunt circuits is quite sensible to the tuning of circuit parameters, little has been published about the complexities in tuning the electric circuit parameters and the effect of the parametric variations on the overall performance of the system (Viana and Steffen, 2006; Andreaus and Porfiri, 2007).

This work presents an analysis of active-passive vibration control using APPN subject to parametric uncertainties in the shunt circuit components, resistance and inductance, and piezoceramic material dielectric and piezoelectric properties. This is done using a recently developed finite element model, which fully accounts for the structure/piezoelectric elements/circuits interaction, combined to stochastic modeling techniques to evaluate confidence intervals for the vibration control performance. Results for the first vibration mode of a cantilever beam with piezoceramic patches connected to active-passive shunt circuits are presented and discussed.

2 FINITE ELEMENT MODEL OF PIEZOELECTRIC SANDWICH BEAMS

A sandwich beam made of piezoelectric layers and modeled using classical sandwich theory was considered. Surface layers and core layer are made of transversely poled and longitudinally poled piezoelectric materials, respectively. Electrodes fully cover the top and bottom skins of all layers so that only through-thickness electric field and displacement are considered. For simplicity, all layers are assumed to be made of orthotropic piezoelectric materials, perfectly bonded and in plane stress state. Bernoulli-Euler theory is retained for the sandwich beam surface layers, while the core is assumed to behave as a Timoshenko beam. It is supposed that each piezoelectric layer can be connected to an electric circuit composed of inductance L_{cj}, resistance R_{cj} and voltage source V_{cj} in series. Based on these assumptions, a two-node beam finite element model was developed with four mechanical and three electrical degrees of freedom per node. The electric displacements in each layer were considered as electrical degrees of freedom. More details on the finite element model can be found in (Santos and Trindade, 2011).

Accounting for equipotentiality on electrodes covering piezoelectric patches surfaces and the relation between electric charges on circuits and patches, the structure-patches-circuits coupled equations of motion can be written as

$$\begin{bmatrix} \mathbf{M} & 0 \\ 0 & \mathbf{L}_c \end{bmatrix} \begin{Bmatrix} \ddot{\mathbf{u}} \\ \ddot{\mathbf{q}}_p \end{Bmatrix} + \begin{bmatrix} \mathbf{C} & 0 \\ 0 & \mathbf{R}_c \end{bmatrix} \begin{Bmatrix} \dot{\mathbf{u}} \\ \dot{\mathbf{q}}_p \end{Bmatrix} + \begin{bmatrix} \mathbf{K}_m & -\bar{\mathbf{K}}_{me} \\ -\bar{\mathbf{K}}_{me}^t & \bar{\mathbf{K}}_e \end{bmatrix} \begin{Bmatrix} \mathbf{u} \\ \mathbf{q}_p \end{Bmatrix} = \begin{Bmatrix} \mathbf{F} \\ \mathbf{V}_c \end{Bmatrix}, \tag{1}$$

where $\mathbf{u}$ and $\mathbf{q}_p$ are the global mechanical displacement and electric charge dofs and $\mathbf{M}$, $\mathbf{K}_m$, $\bar{\mathbf{K}}_{me}$, $\bar{\mathbf{K}}_e$ are the mass and mechanical, piezoelectric and dielectric stiffness matrices and $\mathbf{F}$ is the mechanical force vector. $\mathbf{L}_c$ and $\mathbf{R}_c$ are diagonal matrices containing the inductance and resistance and $\mathbf{V}_c$ is the vector of electric voltage applied to the electric shunt circuits. A structural damping matrix $\mathbf{C}$ can be added a posteriori.

3 PASSIVE AND ACTIVE VIBRATION CONTROL DESIGN

From (1), it is possible to observe that the shunt circuit can affect the structural response either passively through coupling of the dynamics of circuit and structure, via the piezoelectric patches, or actively through the application of an electric voltage in the circuit which excites the structure, also via the piezoelectric patches. These effects can be better observed in a frequency response function (FRF) of the structure when subjected to a mechanical or electrical excitation.

For a purely mechanical excitation, such that $\mathbf{V}_c = 0$ and $\mathbf{F} = \mathbf{b}\tilde{f}e^{\mathrm{j}\omega t}$, the amplitude of a displacement output $y = \mathbf{cu}$ can be written such that $\tilde{y} = G_p(\omega)\tilde{f}$, where the FRF $G_p(\omega)$ is

$$G_p(\omega) = \mathbf{c}\left\{-\omega^2\mathbf{M} + \mathrm{j}\omega\mathbf{C} + \mathbf{K}_m - \bar{\mathbf{K}}_{me}(-\omega^2\mathbf{L}_c + \mathrm{j}\omega\mathbf{R}_c + \bar{\mathbf{K}}_e)^{-1}\bar{\mathbf{K}}_{me}^t\right\}^{-1}\mathbf{b}, \tag{2}$$

from which, it is possible to notice that the resistance and inductance have the effect of changing the dynamic stiffness of the structure. Two particular cases of interest can be derived: i) open-circuit when $\mathbf{R}_c \to \infty$ and ii) short-circuit when $\mathbf{L}_c = \mathbf{R}_c = 0$, in which cases

$$\begin{aligned} G_p^{OC}(\omega) &= \mathbf{c}\left\{-\omega^2\mathbf{M} + \mathrm{j}\omega\mathbf{C} + \mathbf{K}_m\right\}^{-1}\mathbf{b}, \\ G_p^{SC}(\omega) &= \mathbf{c}\left\{-\omega^2\mathbf{M} + \mathrm{j}\omega\mathbf{C} + \mathbf{K}_m - \bar{\mathbf{K}}_{me}\bar{\mathbf{K}}_e^{-1}\bar{\mathbf{K}}_{me}^t\right\}^{-1}\mathbf{b}. \end{aligned} \tag{3}$$

As expected, no structural modification is observed in the open-circuit case while, for the short-circuit case, the stiffness of the piezoelectric patches is reduced.

For a purely electric excitation using a single pair patch-circuit, such that $\mathbf{F} = 0$ and $V_c = \tilde{V}_c e^{\mathrm{j}\omega t}$, the FRF between the output y and the applied voltage V_c is such that $\tilde{y} = G_c(\omega)\tilde{V}_c$, where

$$G_c(\omega) = \mathbf{c}\left\{-\omega^2\mathbf{M} + \mathrm{j}\omega\mathbf{C} + \mathbf{K}_m - \bar{\mathbf{K}}_{me}(-\omega^2 L_c + \mathrm{j}\omega R_c + \bar{K}_e)^{-1}\bar{\mathbf{K}}_{me}^t\right\}^{-1}\bar{\mathbf{K}}_{me}(-\omega^2 L_c + \mathrm{j}\omega R_c + \bar{K}_e)^{-1} \tag{4}$$

In this case, the resistance and inductance of the electric circuit have two effects. The first is a modification on the dynamic stiffness of the structure as in the previous case. The second is a modification of amplitude of the equivalent force input induced in the structure by the applied voltage, which for a properly adjusted circuit can lead to a desirable amplification of the control authority of the pair patch-circuit. The particular case of a simple voltage actuator can be derived by making $L_c = R_c = 0$, for which

$$G_c^V(\omega) = \mathbf{c}\left\{-\omega^2\mathbf{M} + \mathrm{j}\omega\mathbf{C} + \mathbf{K}_m - \bar{\mathbf{K}}_{me}\bar{\mathbf{K}}_e^{-1}\bar{\mathbf{K}}_{me}^t\right\}^{-1}\bar{\mathbf{K}}_{me}\bar{\mathbf{K}}_e^{-1} \tag{5}$$

3.1 Passive vibration control using electromechanical vibration absorbers

Starting from the equations of motion (1) for the case of a single passive electric shunt circuit (RL) connected to a piezoelectric patch embedded in the structure, it is desired to apply the theory of dynamic vibration absorbers for a particular vibration mode of interest. Therefore, the structural response is approximated by the contribution of a single vibration mode of interest such that

$$\mathbf{u}(t) = \phi_n\alpha_n(t), \tag{6}$$

where ϕ_n and α_n are the vibration mode of interest and its corresponding modal displacement. Thus, neglecting the structural damping, the equations of motion for the resulting two degree of freedom system can be written as

$$\begin{aligned} \ddot{\alpha}_n + \omega_n^2\alpha_n - k_p q_p &= b_n f, \\ L_c\ddot{q}_p + R_c\dot{q}_p + \bar{K}_e q_p - k_p\alpha_n &= 0, \end{aligned} \tag{7}$$

where $\phi_n^t\mathbf{M}\phi_n = 1$, $\phi_n^t\mathbf{K}_m\phi_n = \omega_n^2$, $k_p = \phi_n^t\bar{\mathbf{K}}_{me}$ and $b_n = \phi_n^t\mathbf{b}$.

Assuming a mechanical excitation through input f, the structural response measured by a displacement output $y = c_n\alpha_n$, where $c_n = \mathbf{c}\phi_n$, can be written such that its amplitude is $\tilde{y} = G_p(\omega)\tilde{f}$, where the amplitude of the FRF $G_p(\omega)$ is

$$|G_p(\omega)| = c_n b_n\left[(-\omega^2 L_c + \bar{K}_e)^2 + (\omega R_c)^2\right]^{1/2} \times \left\{[\omega^4 L_c - \omega^2(\bar{K}_e + L_c{\omega_n}^2) + \bar{K}_e{\omega_n}^2 - {k_p}^2]^2 + [(-\omega^2 + {\omega_n}^2)\omega R_c]^2\right\}^{-1/2}. \tag{8}$$

For limited values of R_c, $|G_p(\omega)|$ have an anti-resonance at a frequency equal to the resonance frequency of the electrical circuit, defined as $\omega_e = (\bar{K}_e/L_c)^{1/2}$, which can be designed to match the structural resonance of interest ω_n. This leads to an expression for L_c in terms of ω_n, such that

$$L_c = \frac{\bar{K}_e}{\omega_n^2}. \tag{9}$$

From the theory of dynamic vibration absorbers, it is known that the anti-resonance is accompanied by two resonances which may have their amplitudes controlled by the electric circuit resistance R_c. One strategy to design the damping parameter is to minimize the difference between the resonances and anti-resonance amplitudes. This can be done by first using $\lim_{R_c\to 0}|G_p(\omega)|^2 = \lim_{R_c\to\infty}|G_p(\omega)|^2$ to find the frequencies for which the amplitude is independent of damping parameter which are

$$\omega_{1,2}^2 = \frac{1}{2}\left[\omega_e^2 + \omega_n^2 \pm \sqrt{(\omega_e^2 - \omega_n^2)^2 + 2\omega_e^2(k_p^2/\bar{K}_e)}\right]. \tag{10}$$

Equalizing the vibration amplitudes at one of these invariant frequencies ω_1 and at the anti-resonance frequency ω_n leads to an expression for the resistance R_c in terms of the equivalent coupling stiffness k_p, electrical stiffness $\bar{K}_e$ and structural resonance frequency of interest ω_n,

$$R_c = \frac{k_p\sqrt{2\bar{K}_e}}{\omega_n^2}. \tag{11}$$

3.2 Active vibration control using piezoelectric actuators and state feedback

A state feedback LQR (Linear Quadratic Regulator) optimal control is considered. For that, it is necessary to rewrite the equations of motion (1) in state space form, such that a vector of state variables $\mathbf{z}$ is defined, containing the modal displacements and velocities of a series of vibration modes of interest and the electric displacements of the piezoelectric patches and their time-derivatives. This leads to

$$\dot{\mathbf{z}} = \hat{\mathbf{A}}\mathbf{z} + \hat{\mathbf{B}}\mathbf{V}_c + \hat{\mathbf{B}}_f\mathbf{f}\ ,\ \mathbf{y} = \hat{\mathbf{C}}_y\mathbf{z}, \tag{12}$$

where

$$\begin{gathered}\mathbf{z} = \begin{bmatrix} \alpha \\ \mathbf{q}_p \\ \dot{\alpha} \\ \dot{\mathbf{q}}_p \end{bmatrix},\ \hat{\mathbf{A}} = \begin{bmatrix} \mathbf{0} & \mathbf{0} & \mathbf{I} & \mathbf{0} \\ \mathbf{0} & \mathbf{0} & \mathbf{0} & \mathbf{I} \\ -\Omega^2 & \mathbf{K}_p & -\Lambda & \mathbf{0} \\ \mathbf{L}_c^{-1}\mathbf{K}_p^t & -\Omega_e^2 & \mathbf{0} & -\Lambda_e \end{bmatrix}, \\ \hat{\mathbf{B}} = \begin{bmatrix} \mathbf{0} \\ \mathbf{0} \\ \mathbf{0} \\ \mathbf{L}_c^{-1} \end{bmatrix},\ \hat{\mathbf{B}}_f = \begin{bmatrix} \mathbf{0} \\ \mathbf{0} \\ \mathbf{b}_\phi \\ \mathbf{0} \end{bmatrix},\ \hat{\mathbf{C}}_y = [\mathbf{c}_\phi \quad \mathbf{0} \quad \mathbf{0} \quad \mathbf{0}]\,.\end{gathered} \tag{13}$$

The modal displacements are such that $\mathbf{u} = \Phi\alpha$ and, for mass normalized vibration modes, $\Omega^2 = \Phi^t\mathbf{K}_m\Phi$ and $\Lambda = \Phi^t\mathbf{C}\Phi$. Ω is a diagonal matrix which elements are the undamped natural frequencies of the structure with piezoelectric patches in open-circuit. $\Omega_e^2 = \mathbf{L}_c^{-1}\bar{\mathbf{K}}_e$ and $\Lambda_e = \mathbf{L}_c^{-1}\mathbf{R}_c$ are both diagonal matrices which elements stand, respectively, for the squared natural frequencies of the electric circuits and the ratio between the resistances and inductances. The electromechanical coupling stiffness matrix projected in the undamped modal basis is defined as $\mathbf{K}_p = \Phi^t\bar{\mathbf{K}}_{me}$. Input $\mathbf{b}$ and output $\mathbf{c}$ distribution vectors are also defined, with modal projections $\mathbf{b}_\phi = \Phi^t\mathbf{b}$ and $\mathbf{c}_\phi = \mathbf{c}\Phi$, and $\mathbf{f}$ is a vector of the amplitudes of each mechanical force applied to the structure.

A linear state feedback for the applied voltages $\mathbf{V}_c$ is assumed such that $\mathbf{V}_c = -\mathbf{g}\mathbf{z} = -\mathbf{g}_{dm}\alpha - \mathbf{g}_{de}\mathbf{q}_p - \mathbf{g}_{vm}\dot{\alpha} - \mathbf{g}_{ve}\dot{\mathbf{q}}_p$, where $\mathbf{g}$ is a matrix of control gains for each state variable. Therefore, the state space equation (12) becomes

$$\dot{\mathbf{z}} = (\hat{\mathbf{A}} - \hat{\mathbf{B}}\mathbf{g})\mathbf{z} + \hat{\mathbf{B}}_f\mathbf{f}\ ,\ \mathbf{y} = \hat{\mathbf{C}}_y\mathbf{z}. \tag{14}$$

For a single-input mechanical excitation f, the closed-loop or controlled amplitude of a single displacement output y can be written such that $\tilde{y} = G_h(\omega)\tilde{f}$, where the FRF $G_h(\omega)$ is

$$G_h(\omega) = \hat{\mathbf{C}}_y(\mathrm{j}\omega\mathbf{I} - \hat{\mathbf{A}} + \hat{\mathbf{B}}\mathbf{g})^{-1}\hat{\mathbf{B}}_f, \tag{15}$$

which can also be derived from the second order equations of motion projected into the undamped modal basis leading to

$$G_h(\omega) = \mathbf{c}_\phi\left\{-\omega^2\mathbf{I} + \mathrm{j}\omega(\Lambda + \mathbf{K}_p\mathbf{D}_{cc}^{-1}\mathbf{g}_{vm}) + [\Omega^2 + \mathbf{K}_p\mathbf{D}_{cc}^{-1}(\mathbf{g}_{dm} - \mathbf{K}_p^t)]\right\}^{-1}\mathbf{b}_\phi, \tag{16}$$

where the closed-loop dynamic stiffness of the electric circuit $\mathbf{D}_{cc}$ is

$$\mathbf{D}_{cc} = -\omega^2\mathbf{L}_c + \mathrm{j}\omega(\mathbf{R}_c + \mathbf{g}_{ve}) + (\bar{\mathbf{K}}_e + \mathbf{g}_{de}). \tag{17}$$

In this work, the control gain $\mathbf{g}$ is calculated using the standard optimal LQR control theory applied to a single-input/single-output case, that is with only one active-passive patch-circuit pair for the control to minimize the vibration amplitude at one specific location of the structure, such that the following objective function is minimized

$$J = \frac{1}{2}\int_0^\infty \left(\dot{y}^2 + rV_c^2\right)\,\mathrm{d}t, \tag{18}$$

where $\dot{y}$ is the velocity at one location of interest and V_c is the control voltage applied to the active-passive shunt circuit. The weighting factor r is automatically adjusted to guarantee a maximum control voltage of 200 V in all cases following an iterative routine proposed in (Trindade, Benjeddou and Ohayon, 1999).

4 NOMINAL MODEL RESULTS AND DISCUSSION

In this section, the FRFs of cantilever beam configuration, with extension piezoceramic as shown in Figure 1, are analyzed in order to evaluate the APPN performance in terms of passive damping, control authority and active-passive damping. The extension piezoceramics are made of PZT-5H material whose properties are: $\bar{c}_{11}^D = 97.767$ GPa, $\bar{c}_{33}^D = 119.71$ GPa, $c_{55}^D = 42.217$ GPa, $\rho = 7500$ kg m^{-3}, piezoelectric coupling constants $\bar{h}_{31} = -1.3520\ 10^9$ N C^{-1} and

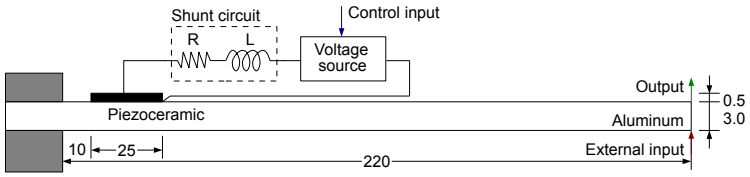

Figure 1: Representation of cantilever beam with piezoceramic patches in extension

$h_{15} = 1.1288\ 10^9$ N C^{-1}, and dielectric constants $\bar{\beta}^{\varepsilon}_{33} = 57.830\ 10^6$ m F^{-1} and $\beta^{\varepsilon}_{11} = 66.267\ 10^6$ m F^{-1}. For the Aluminium beam, material properties are: Young's modulus 70.3 GPa and density 2710 kg m^{-3} and, for the foam, Young's modulus 35.3 MPa, density 32 kg m^{-3} and a viscous damping of 0.5% were considered.

The beam with extension piezoelectric patch is analyzed. The resistance and inductance were tuned to the first resonance frequency, using the methodology developed before (Santos and Trindade, 2011). Notice however that the values obtained using (9) and (11), $R_c = 34117\ \Omega$ and $L_c = 406\ H$, are just a first approximation to the optimal values and had to be fine-tuned manually to $R_c = 31541\ \Omega$ and $L_c = 390\ H$. The purely passive action is obtained by eliminating the voltage source and the purely active action is obtained by making $R_c = L_c = 0$. For the general case, the inductance and resistance not only modify the dynamic stiffness of the structure, leading to damping and/or absorption, but also affects the active control authority of the actuator.

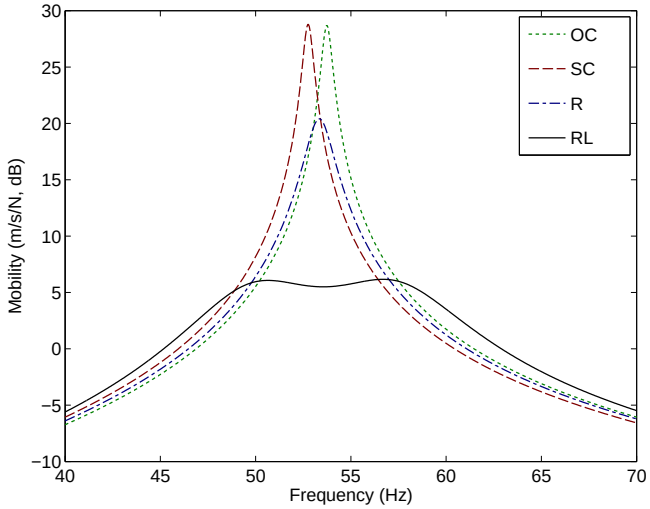

Figure 2: Frequency response of cantilever beam for different circuit conditions: G_p^{OC} (dotted), G_p^{SC} (dashed), G_P^R (dash-dot) and G_p^{RL} (solid).

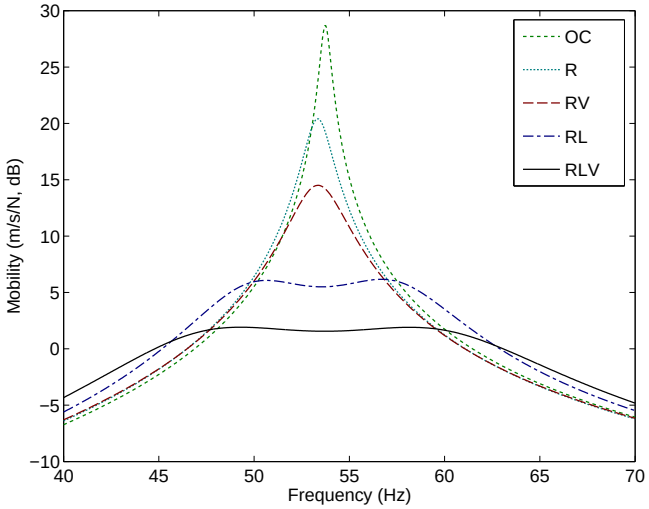

Figure 3: Frequency response of cantilever beam using passive and active-passive shunt circuits: G_p^{OC} (dotted), G_p^R (fine dot), G_h^R (dashed), G_p^{RL} (dash-dot) and G_h^{RL} (solid).

The purely passive performance of resistive and resonant shunt circuits can be evaluated using the frequency response of the beam tip velocity when the beam is subject to a transverse force at the same point (Figure 2). The reference is considered to be unitary. It is possible to observe that both shunt circuits affect significantly only the first resonance, as expected. From which one can conclude that both shunt circuits may yield a vibration amplitude reduction but the resonant circuit leads to a much better performance (approximately 22 dB vibration amplitude reduction). The resistive circuit leads to a variation in the resonance frequency, between short-circuit and open-circuit ones, and also induces an equivalent damping factor. For the resonant circuit, tuning of its resistance allows to reduce amplitude at the structure's resonance frequency (i.e. the anti-resonance of the coupled system) at the cost of increasing the amplitude at the two resonance frequencies of the coupled system.

Then, the LQR state feedback control strategy voltage presented previously was considered to evaluate the control voltage to be applied to the circuit and actively reduce the vibration amplitude of the beam. For uncontrolled beam (open-circuit, $R_c \to \infty$), passive controlled beam with resistive ($R_c = 144\ k\Omega$, $L_c = 0$, $V_c = 0$) and resonant ($R_c = 31541\ \Omega$, $L_c = 390\ H$, $V_c = 0$) shunt circuits, and active-passive controlled beam with resistive ($R_c = 144\ k\Omega$, $L_c = 0$, $V_c < 200\ V$) and resonant ($R_c = 31541\ \Omega$, $L_c = 390\ H$, $V_c < 200\ V$) shunt circuits. As shown in Figure 3, the active-passive control yields better performances than its passive counterpart with amplitude reductions of approximately 14 dB (resistive) and 28 dB (resonant).

5 STOCHASTIC MODELING FOR UNCERTAINTIES ANALYSIS

This section presents an approach for analyzing random uncertainties for dielectric β^{ε}_{33} and piezoelectric $\bar{h}_{31}$ constants of piezoelectric patch and resistance R_c and inductance L_c of the electric shunt circuits. A similar methodology was considered to analyse the effect of uncertainties on each one of these four parameters. An appropriate probabilistic model for each random variable, denoted as X, is constructed accounting for the available information only, which is the following: (1) the support of the probability density function is $]0, +\infty[$; (2) the mean values are such that $E[X] = \underline{X}$; and (3)

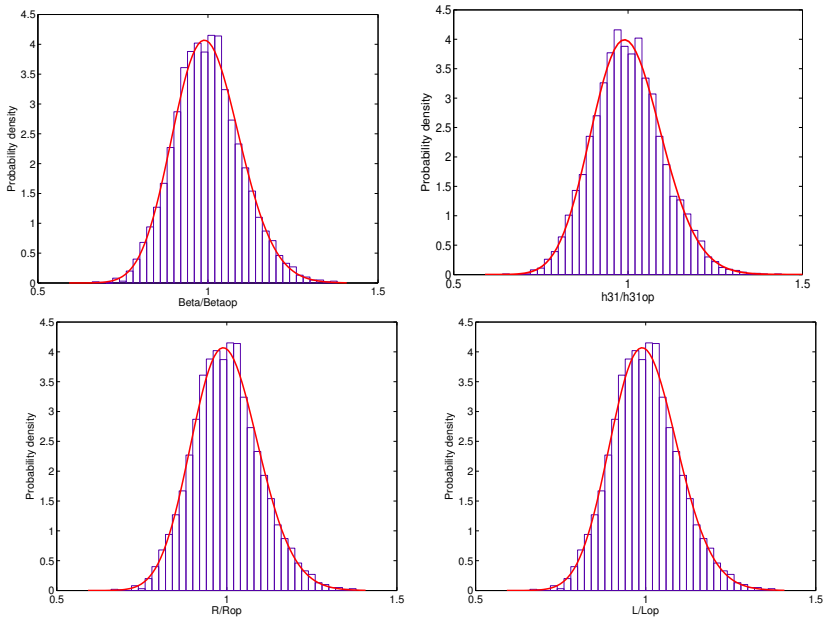

Figure 4: Gamma probability density function and histograms of realizations for material properties $\bar{\beta}^{\varepsilon}_{33}$ and $\bar{h}_{31}$ and circuit parameters R_c and L_c.

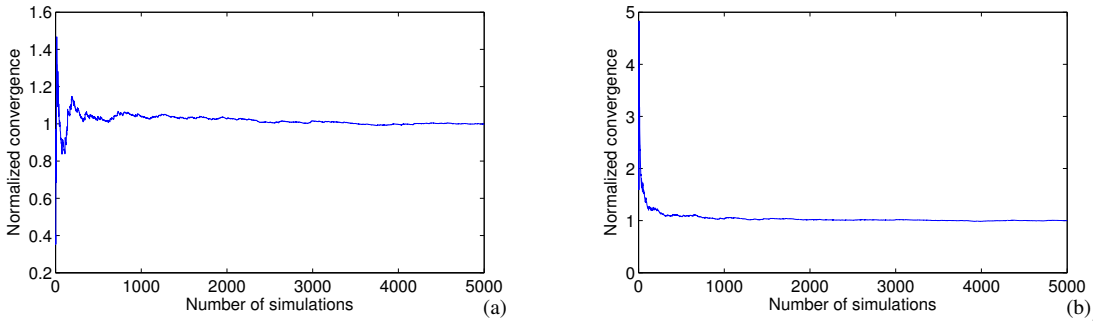

Figure 5: Mean square convergence of Monte Carlo simulations considering as uncertain parameters: (a) only L_c and (b) $\bar{\beta}^{\varepsilon}_{33}$, $\bar{h}_{31}$, R_c and L_c simultaneously.

zero is a repulsive value for the positive-valued random variables which is accounted for by the condition $E[ln(X)] = c_X$ with $|c_X < +\infty$. Therefore, the Maximum Entropy Principle yields the following Gamma probability density functions for X (Soize, 2001; Cataldo et al., 2009; Ritto et al., 2010).

$$p_X(X) = \mathbb{I}_{]0,+\infty[}(X)\frac{1}{\underline{X}}\left(\frac{1}{\delta_X^2}\right)^{\delta_X^{-2}}\frac{1}{\Gamma(\delta_X^{-2})}\left(\frac{X}{\underline{X}}\right)^{\delta_X^{-2}-1}\exp\left(-\frac{X}{\delta_X^2\underline{X}}\right) \tag{19}$$

in which $\delta_X = \sigma_X/\underline{X}$ is the relative dispersion of $\widehat{X}$ and σ_X are their standard deviations. The Gamma function is defined as $\Gamma(\alpha) = \int_0^{\infty} t^{\alpha-1}e^{-t}\mathrm{d}t$. These probability density functions are shown in Figure 4 together with the histograms of random sets for each variable generated with MATLAB function *gamrnd*, considering 5000 realizations. The vectors of random realizations for $\widehat{X}$, when considering all four parameters simultaneously, where combined and then applied to the evaluation of realizations of the FRFs $G_p(\theta_j,\omega)$, $G_c(\theta_j,\omega)$ and $G_h(\theta_j,\omega)$ using equations (2), (4) and (15), respectively.

The mean-square convergence analysis with respect to the independent realizations of random variable $\widehat{G}_p(\omega)$, denoted by $G_p(\theta_j,\omega)$ was carried out considering the function

$$conv(n_s) = \frac{1}{n_s}\sum_{j=1}^{n_s}\int \|G_p(\theta_j,\omega) - G_p^N(\omega)\|^2\,\omega, \tag{20}$$

where n_s is the number of simulations and $G_p^N(\omega)$ is the response calculated using the corresponding mean model. Figures 5 shows the mean-square convergence analysis for extension configuration considering $\delta_X = 0.10$. It is possible to observe that for both cases 3000 simulations are enough to assure convergence. Despite that, the statistical analyses presented in the following sections consider all 5000 simulations performed.

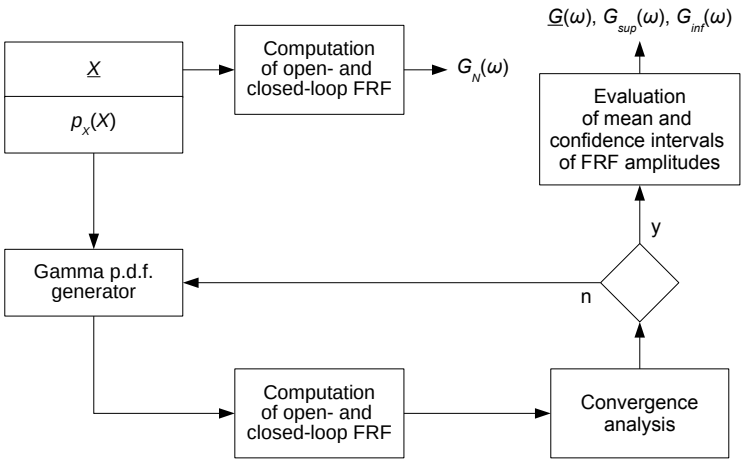

Figure 6: Schematic procedure for the computation of FRFs mean and confidence intervals.

The statistical analyses of the FRF amplitudes were performed using their 5000 realizations at each frequency to calculate the corresponding mean values and 95% confidence intervals. The 95% confidence intervals were evaluated using the 2.5% and 97.5% percentiles of the realizations of FRF amplitudes at each frequency. Figure 6 summarizes the simulation procedure.

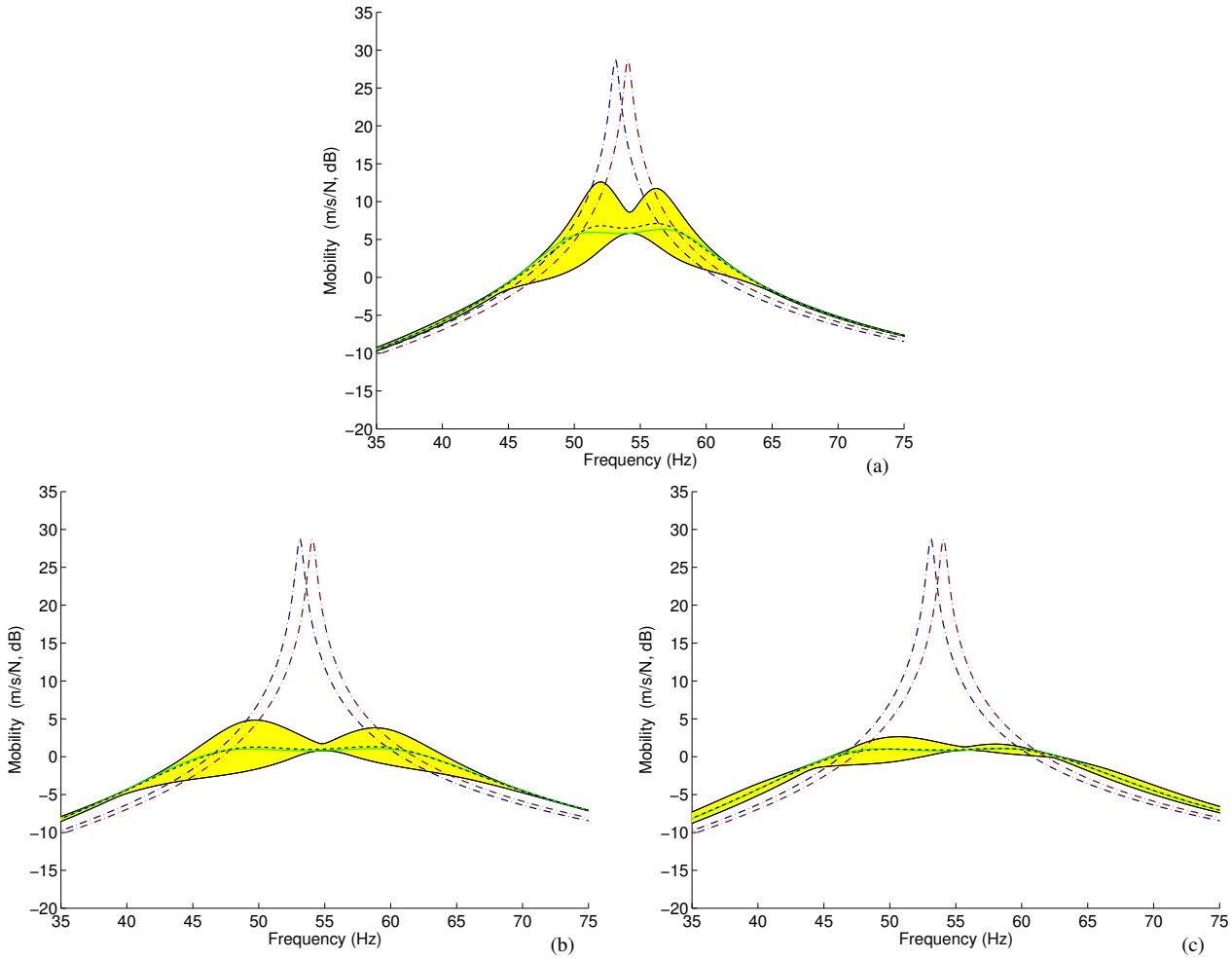

Figure 7: Mean (dashed) and nominal (solid) values and 95% confidence interval (filled) for the frequency response of the controlled cantilever beam, as compared to OC and SC conditions (dash-dot), subjected to uncertainties in $\bar{\beta}^{\varepsilon}_{33}$. (a) Passive shunt, (b) active-passive shunt with constant control gain, and (c) active-passive shunt with updated control gain.

As a first analysis, the dielectric constant $\bar{\beta}^{\varepsilon}_{33}$ alone is considered as uncertain according to the Gamma probability density function described previously. The other three parameters are fixed at their nominal values. Figure 7 shows the

mean, nominal and 95% confidence interval for the frequency response of the controlled cantilever beam subjected to uncertainties of dielectric constant when using purely passive shunt (open-loop) and active-passive shunt with constant and variable (updated) control gains. A dispersion of 10% was considered for the dielectric constant and its mean value coincides with the nominal value $\bar{\beta}_{33}^{\varepsilon} = 57.830\ 10^6$ m F^{-1}. Since it was observed that, as expected, the RL shunt circuit only affects the frequency response near the first resonance (for which the shunt circuit was designed), Figure 7 is zoomed near the first resonance. One may notice, from Figure 7a, that the nominal model indicates a passive reduction in the vibration amplitude of 22 dB (considering the difference between peak responses for OC and RL), while when considering the uncertainties of dielectric constant this reduction is found to be in the range 16-23 dB. It can be noticed also that the difference between the mean and nominal FRFs is almost negligible.

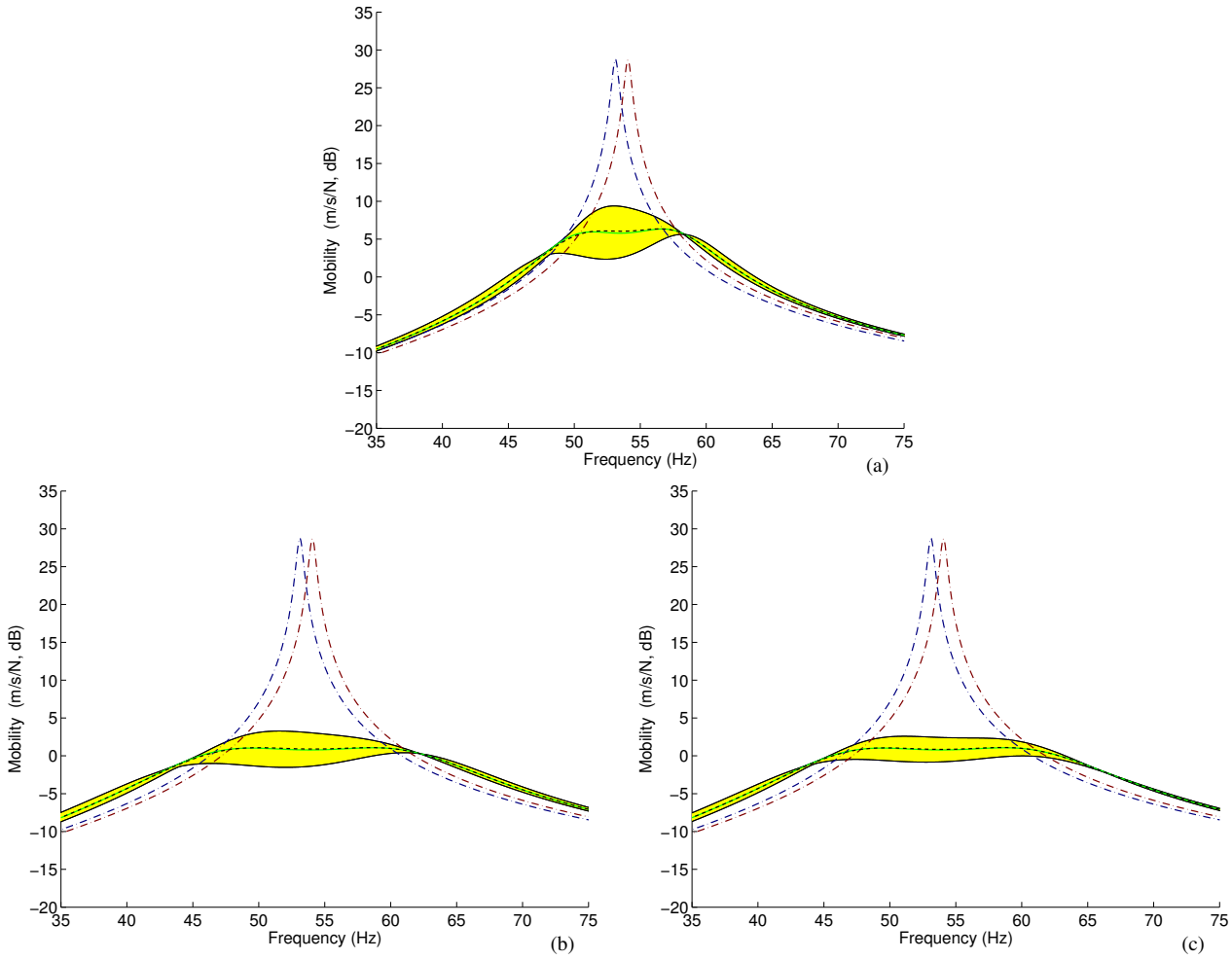

Figure 8: Mean (dashed) and nominal (solid) values and 95% confidence interval (filled) for the frequency response of the controlled cantilever beam, as compared to OC and SC conditions (dash-dot), subjected to uncertainties in $\bar{h}_{31}$. (a) Passive shunt, (b) active-passive shunt with constant control gain, and (c) active-passive shunt with updated control gain.

An analysis of the active-passive vibration control performance may also be observed in Figures 7b and 7c, which shows the frequency response of uncontrolled (G_p^{OC}) and controlled structure (G_h^N), including the mean and confidence intervals. Figures 7b and 7c show that LQR control combined with the resonant shunt circuit allows to reduce further the vibration amplitude. In the first case (Figure 7b), the control gain vector is fixed at its nominal value while, in the second case (Figure 7c), the control gain is updated (reevaluated) for each realization of the uncertain parameter, which is only possible if the dielectric parameter although uncertain could be measured and used to evaluate the control gain. The nominal model indicates a active-passive reduction in the vibration amplitude of 27.5 dB, while the confidence intervals indicate a reduction between 24 and 28 dB for fixed control gain (Figure 7b) and between 26 and 28 dB for updated control gain (Figure 7c).

A similar analysis was performed considering the piezoelectric constant $\bar{h}_{31}$ as an uncertain parameter, with 10% dispersion and $\bar{h}_{31} = -1.3520\ 10^9$ N C^{-1} mean value. It is expected that the higher the piezoelectric constant the higher the vibration amplitude reduction, since this constant affects directly the electromechanical coupling and, thus, the energy conversion efficiency. From Figure 8a, one may notice that while the nominal model indicates a reduction in the vibration amplitude of 22 dB, the piezoelectric constant uncertainties lead to a peak-to-peak amplitude reduction confidence interval similar to the previous case (19-23 dB), although the shape of the confidence interval near the first resonance is quite different from the previous one (Figure 7a). The 95% confidence intervals for the active-passive control indicate a

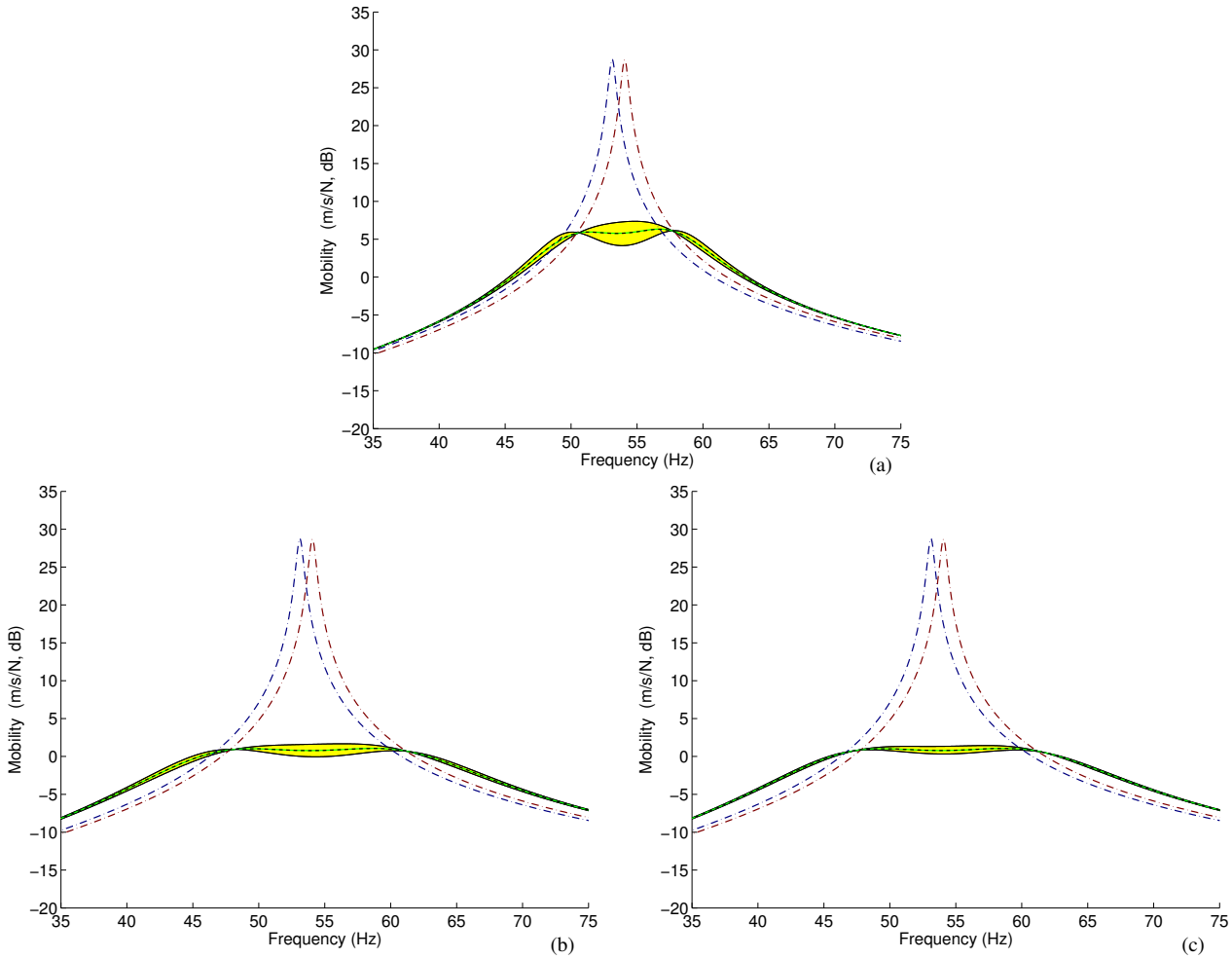

Figure 9: Mean (dashed) and nominal (solid) values and 95% confidence interval (filled) for the frequency response of the controlled cantilever beam, as compared to OC and SC conditions (dash-dot), subjected to uncertainties in R_c. (a) Passive shunt, (b) active-passive shunt with constant control gain, and (c) active-passive shunt with updated control gain.

reduction between 25 and 28 dB using a fixed control gain (Figure 8b) and between 26 and 29 dB using updated control gain (Figure 8c), compared to the nominal amplitude reduction of 27.5 dB.

As for the electric shunt circuit components, the resistance and inductance were then considered as uncertain parameters. In both cases, a dispersion of 10% is considered. The mean values for resistance and inductance are $R_c = 31541\ \Omega$ and $L_c = 390\ H$, respectively. In the case of an uncertain resistance, the passive vibration amplitude reduction may be in the range 21-23 dB (Figure 9), compared to a nominal value of 22 dB. For the active-passive vibration control, the vibration amplitude reduction is in the range 27-29 dB, using fixed control gain (Figure 9b), or in the range 27-28 dB, using updated control gain (Figure 9c). These results show that the vibration control performance, both passive and active-passive, is much less sensitive to the resistance of the shunt circuit. The resistance uncertainties affect mainly the frequency response at resonance frequency.

On the other hand, the effect of uncertainties of shunt circuit inductance is much more important. As shown in Figure 10, the 95% confidence intervals of the frequency response near the first resonance are similar to those observed in Figure 7 corresponding to uncertainties of dielectric constant. Both parameters affect the shunt electric circuit resonance frequency and thus the proper tuning between the target frequency (structural resonance frequency) and the electric circuit resonance frequency. This mistuning seems to have also a greater effect on the peak-to-peak vibration amplitude reduction. The predicted passive reduction stands between 16 and 23 dB (Figure 10a), while the active-passive one is in the range 24-28 dB (Figure 10b), for fixed control gain, and 26-28 dB, for updated control gain (Figure 10c).

Finally, it is worthwhile to analyse the effect of uncertainties of the four parameters simultaneously on the passive and active-passive vibration amplitude reduction. Both dispersion and mean values are the same as the ones used in the individual analyses. In this case, a wider confidence interval should be expected. Indeed, as shown in Figure 11, both passive and active-passive vibration control performance are affected around the first resonance. The inductance and dielectric constant affect the amplitude mainly near the invariant frequencies, the resistance affect the amplitude mainly near the resonance frequency and the piezoelectric constant affect the amplitude over a wider frequency range. Thus, the combination of the four parametric uncertainties effects leads to a more spreaded variation of the amplitude reduction. Considering the peak-to-peak vibration amplitude reduction, the stochastic model predicts an amplitude reduction between 14 and 26 dB, for the passive shunt (Figure 11a), between 22 and 29 dB, for active-passive shunt with fixed control gain

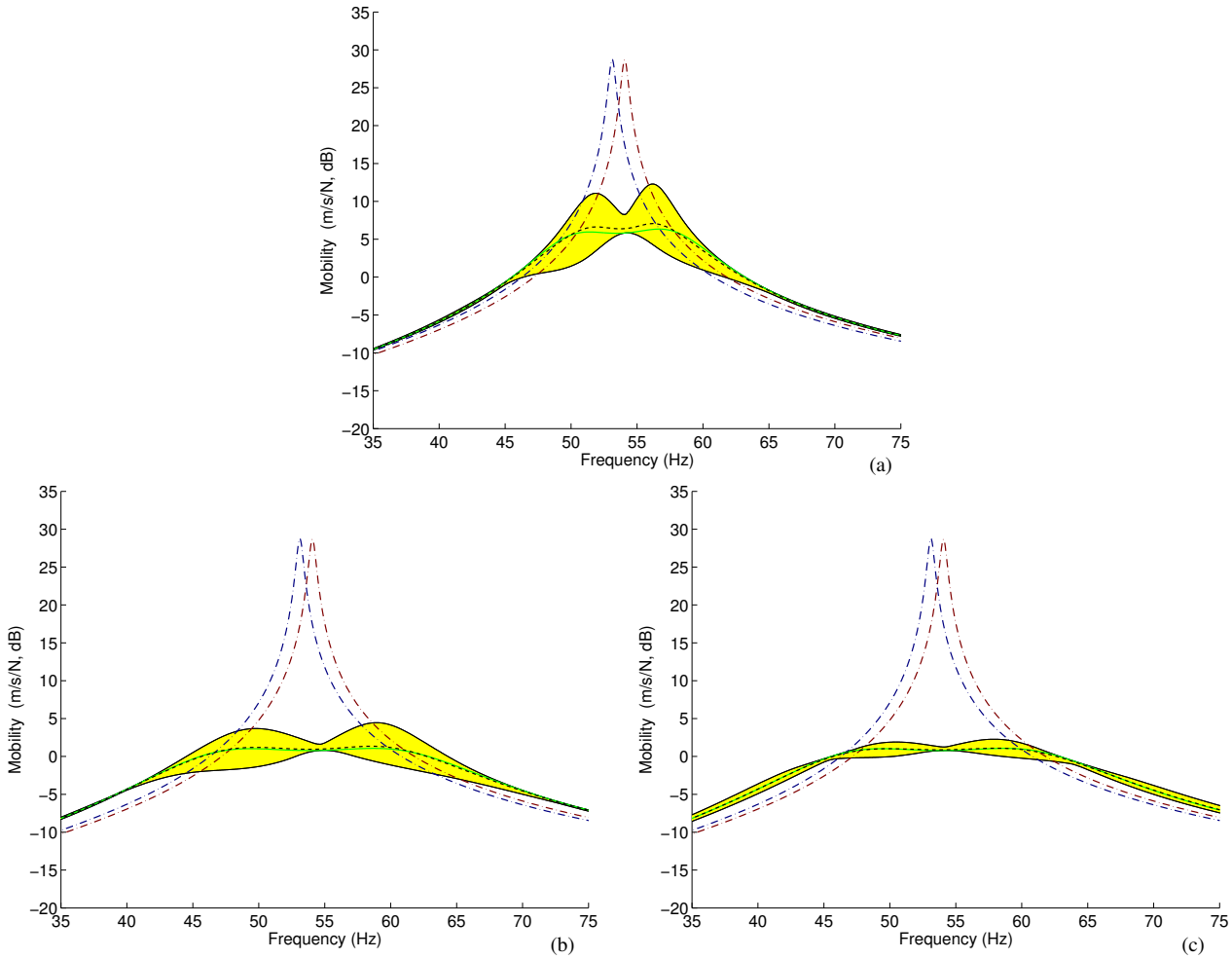

Figure 10: Mean (dashed) and nominal (solid) values and 95% confidence interval (filled) for the frequency response of the controlled cantilever beam, as compared to OC and SC conditions (dash-dot), subjected to uncertainties in L_c. (a) Passive shunt, (b) active-passive shunt with constant control gain, and (c) active-passive shunt with updated control gain.

(Figure 11b), and between 25 and 29 dB, for active-passive shunt with updated control gain (Figure 11c).

6 CONCLUSIONS

This work has presented an analysis of active-passive vibration control using Active-Passive Piezoelectric Networks subject to parametric uncertainties in the shunt circuit components and piezoelectric material properties. This was done using a finite element model, which fully accounts for the structure/piezoelectric elements/circuits interaction, combined to stochastic modeling techniques to evaluate confidence intervals for the vibration control performance. Results for the first vibration mode of a cantilever beam with piezoceramic patches connected to active-passive shunt circuits were presented and discussed. It was shown that the inductance and dielectric constant affect the amplitude mainly near the invariant frequencies, the resistance affect the amplitude mainly near the resonance frequency and the piezoelectric constant affect the amplitude over a wider frequency range. Thus, the combination of the four parametric uncertainties effects leads to a more spreaded variation of the amplitude reduction. Considering the peak-to-peak vibration amplitude reduction, the stochastic model predicts an amplitude reduction between 14 and 26 dB, for the passive shunt, between 22 and 29 dB, for active-passive shunt with fixed control gain, and between 25 and 29 dB, for active-passive shunt with updated control gain.

ACKNOWLEDGEMENTS

The first author acknowledges CAPES for a graduate scholarship. The authors also acknowledge the support of the MCT/CNPq/FAPEMIG National Institute of Science and Technology on Smart Structures in Engineering, grant no.574001/2008-5.

7 REFERENCES

Andreaus, U. and Porfiri, M., 2007, “Effect of electrical uncertainties on resonant piezoelectric shunting,” Journal of Intelligent Material Systems and Structures, Vol.18, pp.477–485.

Baillargeon, B.P. and Vel, S.S., 2005, “Active vibration suppression of sandwich beams using piezoelectric shear ac-

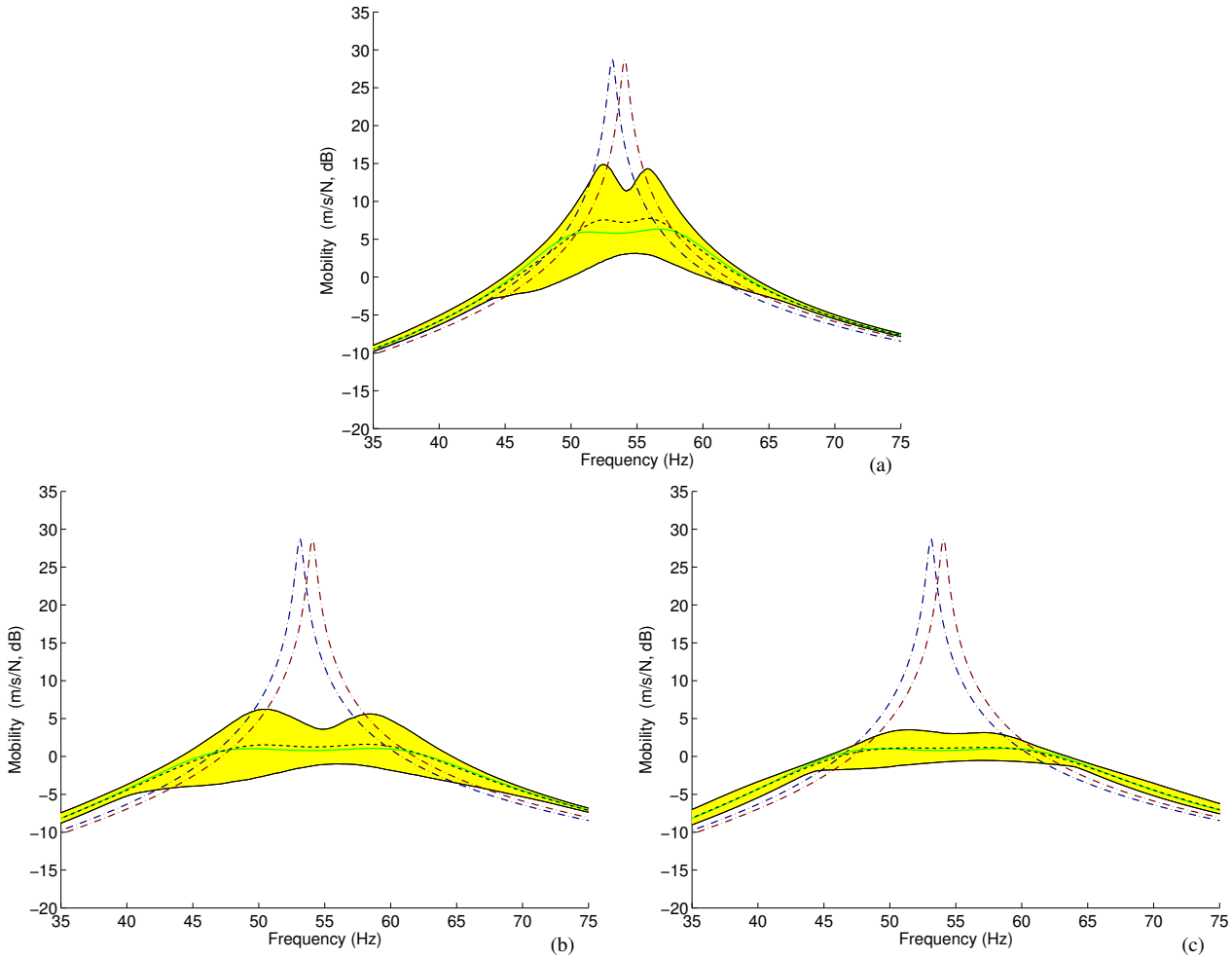

Figure 11: Mean (dashed) and nominal (solid) values and 95% confidence interval (filled) for the frequency response of the controlled cantilever beam, as compared to OC and SC conditions (dash-dot), subjected to uncertainties in the four parameters. (a) Passive shunt, (b) active-passive shunt with constant control gain, and (c) active-passive shunt with updated control gain.

tuators: experiments and numerical simulations," Journal of Intelligent Materials Systems and Structures, Vol.16, No.6, pp.517–530.

Benjeddou, A., 2007, "Shear-mode piezoceramic advanced materials and structures: a state of the art," Mechanics of Advanced Materials and Structures, Vol.14, No.4, pp.263–275.

Benjeddou, A. and Ranger-Vieillard, J.-A., 2004, "Passive vibration damping using shunted shear-mode piezoceramics," In Topping, B.H.V. and Mota Soares, C.A., eds., Proceedings of the Seventh International Conference on Computational Structures Technology, Civil-Comp Press, Stirling, Scotland, p.4.

Benjeddou, A., Trindade, M.A., and Ohayon, R., 1999, "New shear actuated smart structure beam finite element," AIAA Journal, Vol.37, No.3, pp.378–383.

Cataldo, E., Soize, C., Sampaio, R. and Desceliers, C., 2009, "Probabilistics modeling of a nonlinear dynamical system used for producing voice," Computational Mechanics, Vol.43, pp.265275

Forward, R., 1979, "Electronic damping of vibrations in optical structures," Applied Optics, Vol.18, No.5, pp.690–697.

Hagood, N.W. and von Flotow, A., 1991, "Damping of structural vibrations with piezoelectric materials and passive electrical networks," Journal of Sound and Vibration, Vol.146, No.2, pp.243–268.

Raja, S., Prathap, G., and Sinha, P.K., 2002, "Active vibration control of composite sandwich beams with piezoelectric extension-bending and shear actuators," Smart Materials and Structures, Vol.11, No.1, pp.63–71.

Ritto, T., Soize, C., Sampaio, R., 2010, "Stochastic dynamics of a drill-string with uncertain weight-on-hook," Journal of the Brazilian Society of Mechanical Sciences and Engineering, Vol.32, No.3, pp.250-258.

Santos, H.F.L. and Trindade, M.A., 2011, "Structural Vibration Control Using Extension and Shear Active-Passive Piezoelectric Networks Including Sensitivity to Electrical Uncertainties,"Journal of the Brazilian Society of Mechanics Science and Engineering, Vol.33, No.3, pp.287-301.

Soize, C., 2001, "Maximum entropy approach for modeling random uncertainties in transient elastodynamics," Journal of the Acoustical Society of America, Vol.109, No.5, pp.1979–1996.

Sun, C.T. and Zhang, X.D., 1995, "Use of thickness-shear mode in adaptive sandwich structures," Smart Materials and Structures, Vol.4, No.3, pp.202–206.

Thornburgh, R.P., and Chattopadhyay, A., 2003, "Modeling and optimization of passively damped adaptive composite structures," Journal of Intelligent Materials Systems and Structures, Vol.14, No.4-5, pp.247–256.

Trindade, M.A. and Benjeddou, A., 2006, "On higher-order modelling of smart beams with embedded shear-mode piezoceramic actuators and sensors," Mechanics of Advanced Materials and Structures, Vol.13, No.5, pp.357–369.

Trindade, M.A. and Benjeddou, A., 2009, "Effective electromechanical coupling coefficients of piezoelectric adaptive structures: critical evaluation and optimization," Mechanics of Advanced Materials and Structures, Vol.16, No.3, pp.210–223.

Trindade, M.A., Benjeddou, A., and Ohayon, R., 1999, "Parametric analysis of the vibration control of sandwich beams through shear-based piezoelectric actuation," Journal of Intelligent Materials Systems and Structures, Vol.10, No.5, pp.377–385.

Trindade, M.A., Benjeddou, A., and Ohayon, R., 2001, "Finite element modeling of hybrid active-passive vibration damping of multilayer piezoelectric sandwich beams – part 2: System analysis," International Journal for Numerical Methods in Engineering, Vol.51, No.7, pp.855–864.

Trindade, M.A. and Maio, C.E.B., 2008, "Multimodal passive vibration control of sandwich beams with shunted shear piezoelectric materials," Smart Materials and Structures, Vol.17, art.no.055015.

Tsai, M.S., and Wang, K.W., 1999, "On the structural damping characteristics of active piezoelectric actuators with passive shunt," Journal of Sound and Vibration, Vol.221, No.1, pp.1–22.

Viana, F.A.C. and Steffen Jr., V., 2006, "Multimodal vibration damping through piezoelectric patches and optimal resonant shunt circuits," Journal of the Brazilian Society of Mechanical Sciences and Engineering, Vol.28, No.3, pp.293–310.

RESPONSIBILITY NOTICE

The authors are the only responsible for the printed material included in this paper.